Available online at www.sciencedirect.com
ScienceDirect
Journal of Environmental Sciences 2012, 24(3) 479–487
JOURNAL OF ENVIRONMENTAL SCIENCES
ISSN 1001-0742
CN 11-2629/X
www.jesc.ac.cn

Photocatalytic degradation of 4-chlorophenol under P-modified TiO_2/UV system: Kinetics, intermediates, phytotoxicity and acute toxicity

Kais Elghniji[1], Olfa Hentati[1,2], Najwa Mlaik[1], Ayman Mahfoudh[2], Mohamed Ksibi[1,2,*]

1. University of Sfax, Laboratoire Eau, Energie et Environnement ENIS, B.P 1173, 3038 Sfax, Tunisia
2. Institut Supérieur de Biotechnologie de Sfax B.P 1175, 3038 Sfax, Tunisia. E-mail : mohamed.ksibi@tunet.tn

Received 25 February 2011; revised 22 April 2011; accepted 05 May 2011

Abstract

A series of phosphorus-modified titanium dioxide samples with varying P/Ti atomic ratio were conveniently prepared via a conventional solgel route. The effects of phosphorus content and calcination temperature on the crystalline structure, grain growth, surface area, and the photocatalytic activity of P-modified TiO_2 were investigated. The XRD results showed that P species slow down the particle growth of anatase and increase the anatase-to-rutile phase transformation temperature to more than 900°C. Kinetic studies on the P-modified TiO_2 to degraded 4-chlorophenol had found that the $TP5_{500}$ prepared by adopting a P/Ti atomic ratio equal to 0.05 and calcined at 500°C had an apparent rate constant equal to 0.0075 min^{-1}, which is superior to the performance of a commercial photocatalyst Degussa P25 K_{app} = 0.0045 min^{-1} and of unmodified TiO_2 ($TP0_{500}$) K_{app} = 0.0022 min^{-1}. From HPLC analyses, various hydroxylated intermediates formed during oxidation had been identified, including hydroquinone (HQ), benzoquinone (BQ) and (4CC) 4-chlorocatechol as main products. Phytotoxicity was assessed before and after irradiation against seed germination of tomato (*Lycopersicon esculentum*) whereas acute toxicity was assessed by using *Folsomia candida* as the test organism. Intermediates products were all less toxic than 4-chlorophenol and a significant removal of the overall toxicity was accomplished

Key words: P-modified TiO_2; photocatalyst; 4-chlorophenol; acute toxicity; germination

DOI: 10.1016/S1001-0742(10)60659-6

Introduction

Chlorophenols constitute a group of serious environmental pollutants that must be eliminated. As a result of their widespread use in mothproofing, miticides, pesticides, herbicides, germicides, fungicides and wood preservation, chlorophenols pose a serious threat to the environment. Chlorophenols can be found in surface water, soil, industrial water, ecosystems and human beings (Poulios et al., 1999; Peng et al., 2006). The US Environmental Protection Agency (US EPA, 1987) and the European Union directive (EEC, 1990) have labelled chlorophenols as "priority pollutants", which means that they need to be constantly monitored in the aquatic environment and that a value of 0.5 mg/L is the upper permissible limit of these compounds in publicly supplied water. The removal of this compound from wastewaters is currently performed by conventional treatment methods, such as biological treatment, chlorination and adsorption. However, the biological process usually requires a considerably long treatment time to break down organic pollutants leading to an unacceptable level of 4-chlorophenol in the final effluent. Chlorination poses another problem since it often generates carcinogenic by-products. Granular activated carbon adsorption is another commercialized process but the spent carbon needs to be disposed (Chen and Ray, 1999). Alternative methods to these well-established techniques to remove theses toxicants are the so-called advanced oxidation processes (AOPs) (Scott and Ollis, 1995; Herrmann et al., 1999; Pera-Titius et al., 2004) which have been reported to be effective for the degradation of soluble organic contaminants from waters and soils providing almost total degradation. Several technologies are included in the AOPs like photo-Fenton, ozonation, photocatalysis, etc. These processes are based on the generation of the strongly oxidizing hydroxyl radicals (OH), which oxidize a broad range of organic pollutants that could be present in water and wastewaters. Among these technologies, heterogeneous photocatalysis is placed in the forefront of vigorous research activity due to its efficiency of total destruction of pollutants, non-selectivity and the formation of benign products.TiO_2 mediated heterogeneous photocatalysis has been proved to be potentially advantageous as it may proceed at ambient conditions and lead to the complete mineralization of many organic pollutants to harmless products of CO_2, H_2O and mineral acids (Cheng et al., 2007). Both of its crystal structures, anatase and rutile, are extensively used as photocatalysts (Tanaka et al., 1991; Fujishima et al., 2000). In most reactions, anatase exhibits higher photocatalytic

* Corresponding author. E-mail: mohamed.ksibi@tunet.tn

activity which is probably due to its slightly higher Fermi level and its higher surface density of hydroxyl groups (Bickley et al., 1991). Anatase-TiO_2 is metastable and transforms to the rutile, a thermodynamic stable state, upon heating (Gerischer and Heller, 1992). The anatase-to-rutile phase transformation of TiO_2 greatly reduces surface areas of the particles (Ding et al., 2000; Chen et al., 2001), which may result in an inhibition in photocatalytic ability of TiO_2. Accordingly, increasing stability temperature range of the anatase phase of the TiO_2 nanoparticles is vital in enhancing the photocatalytic abilities and broadening the applications of TiO_2. The most promising methods that include surface modifications by doping with anionic ion such as phosphate. In fact, this specie tends to retard the phase transition of anatase to rutile, increase the surface area and consequently enhance the photocatalytic activity (Yu et al., 2003; Chang et al., 2009).

In this article, we investigated the performance P-modified TiO_2 catalysts in the photocatalytic of 4-chlorophenol under UV irradiation. The effect of phosphorous content on the thermal stability and the crystal growth properties was investigated. The results in terms of 4-chlorophenol removal, organics mineralization, intermediates produced, and their respective phytotoxicity and acute toxicity were useful to assess the feasibility of the treated solution in the environment.

1 Material and methods

1.1 Powder preparation

The sol-gel approach was used to prepare both unmodified and P-modified TiO_2 catalysts. The former preparation started from the reaction of a solution of titanium(IV) isopropoxide in isopropylic alcohol (molar ratio 1:4). Deionized water was added dropwise to $Ti(OPri)_4$ solution during stirring (molar ratio between water and alcohol 1:5). White precipitate starts appearing indicating the hydrolysis process. After being aged for an hour, 100 mL of aqueous solution of 85% purity H_3PO_4 (Aldrich, USA) with various concentrations (16, 34.5 and 55 mmol/L) was added to the resulting titania suspension to prepare TiO_2 samples of varied phosphorus content, atomic ratios employed are P/Ti = 0.025, 0.05, and 0.08. For comparison, unmodified TiO_2 was also prepared by the same procedure without the addition of H_3PO_4. The gel obtained was aged overnight at room temperature then dried at 70°C which are denoted P8, P5, and P2.5 corresponding to P/Ti atomic ratios of 0.08; 0.05; and 0.025 respectively. Unmodified gel of titania is denoted P0. The dried materials were calcined in air for 3 hr and with heating rate 10°/min. The calcined powders were denoted $TP8_{Y00}$, $TP5_{Y00}$, $TP2.5_{Y00}$ and $TP0_{Y00}$ with the respect of calcination temperature, Y00 equal to 500, 700, 900 and 1000°C.

1.2 Sample characterization

The powder X-ray diffraction patterns were recorded at room temperature on a X-ray diffractometer (D8 advance, Bruker, Germany). The data were collected in the 2θ range 2–70° with a step size of 0.02° and a counting time of 5 sec/step. The Brunauer-Emmett-Teller (BET) surface area was measured by a fully automated surface area analyzer (ASAP 2020 Accelerated Surface Area and Porosimetry, Micromeritics, USA). The samples were degassed in vacuum overnight at 180°C prior to adsorption measurements. Infrared absorption spectra were measured on a spectrometer (Nicolet 380 ATR/FT-IR, International Equipment Trading Ltd., USA) by the transmission method using the KBr pellet technique with 4 cm^{-1} resolution. The Ti and P content of the samples were determined using an inductively coupled plasma argon emission spectrometer (ICP-AES, Thermo Jarrell ASH, USA). Prior to analyse, 20 mg of P-modified TiO_2 samples was transferred into Teflon flask and then completely dissolved in a fluorhydric acid/nitric acid mixture (28%/68% in volume) solution using a microwave (CEM, MARS 5). After dissolution, the mixture was diluted with 100 mL of deionized water and analyzed by ICP-AES. The intensity of the spectral lines of 213.6 nm (phosphorus) and 336.1 nm (titanium) were measured. Results are corrected for spectral inter-element interferences.

1.3 Photocatalytic reaction experiment

Figure 1 represents the laboratory-scale photoreactor used for the photodegradation of 4-chlorophenol. It is a 120-cm^3 cylindrical photoreactor, operating in a closed recirculating circuit driven by a centrifugal pump and with a stirred reservoir tank equipped with a device for withdrawal of samples. Illumination was carried out using a 11-W low-pressure mercury lamp (Philips, Holland) with a wavelength in the range of 200–280 nm. The concentrations of 4-chlorophenol and intermediate products in the filtered sample were determined by a high performance liquid chromatography (HPLC, Knauer, Germany) equipped with an UV detector and the RP-C18 (eurosphere-100) column (220 mm length, 4.6 mm inner diameter). Substances were quantified from their absorbance at 220 and 280 nm. Methanol-water mobile phase in the ratio of 60%–40% (*V/V*) was used in isocratic elution at flow rate of 1 mL/min. Free chloride ions were quantified directly after each irradiation period with an ion chromatograph (HIC-6A Shimadzu, Japan) equipped with a conductivity detector and a Shim-pack column. The separation was achieved using an isocratic elution at a flow rate of 1.5 mL/min. A mobile phase of 1 mmol/L of tris(hydroxymethyl)aminomethane and 1 g/L of sodium chloride was used as standards solution. Total organic carbon (TOC) was measured using a TOC analyzer (TOC-5000A, Shimadzu, Japan) (catalytic oxidation on Pt at 680°C) via calibration using standards of potassium phthalate. Chemical oxygen demand (COD) and biological oxygen demand (BOD) were measured according to standard methods described in the Japanese International Standard Handbook (JIS, 1998).

1.4 Germination tests

4-Chlorphenol phytotoxicity was assessed before and after irradiation against seed germination of tomato (*Lycoper-*

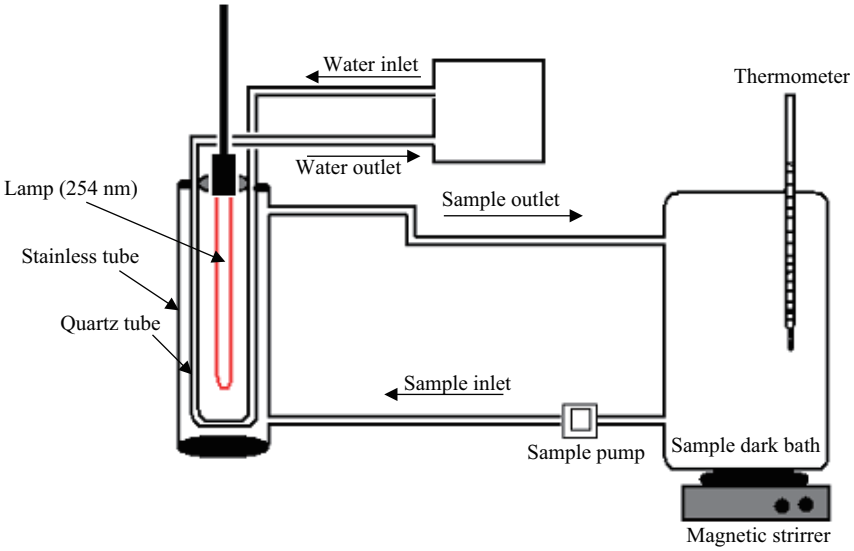

Fig. 1 Photocatalytic reactor system for 4-chlorophenol degradation with UV lamp.

sicon esculentum). Phytotoxicity was determined using a modified Zucconi test (Zucconi et al., 1981) by measuring seed germination. Twenty seeds were placed on filter papers in 9 cm Petri dishes and 6 mL of treated solution were then uniformly added to each dish. Dishes were incubated in the dark at (26 ± 2)°C for 5 days. Distilled water was used as control. All samples, including controls, were triplicated. A germination index (GI) was calculated by counting the number of germinated seeds and the average root length observed in each sample compared to control treatments (Komilis et al., 2005). Results finally expressed according to the following equation:

$$GI = \frac{Ns}{Nc} \times \frac{Ls}{Lc} \times 100\%$$

where, *N*s and *N*c are numbers of germination seeds in sample and control, respectively, and *L*s and *L*c are average of root lengths in sample and control, respectively.

A seed was considered germinated when the root length exceeded 5 mm. For root lengths below 5 mm, it was considered equal to 0 and the seed was not considered germinated. The average sum of root lengths comprised the sum of the lengths of all germinated seeds in a Petri dish.

1.5 Avoidance tests with collembolans Folsomia candida

The avoidance tests with the springtails were based on International Organization for Standardization Guideline ISO 11267 (1999), although several modifications were performed to the protocol to adapt it to the experimental aims and waste properties. The Folsomia candida culture used in the tests was raised in our laboratory and was initiated one year ago from cultures of the Instituto do Mar-IMAR University of Coimbra (Portugal). Cultures were raised in polyethylene containers (17.5 cm × 12.5 cm × 7.5 cm). The substrate consisted of a 1 cm layer of a wet mixture of plaster of Paris and charcoal (9:1, *V*/*V*). Cultures were raised in darkness in a climatic chamber at a constant temperature of 21°C. The substrate was renewed and the density of individuals was reduced every two months to avoid overcrowding. Five samples issues from the photocatalytic treatment of 4-chlorophenol solution were used. These samples correspond to 0, 45, 90, 150 and 270 min irradiation time. The residual 4-chlorophenol solutions were mixed with OECD artificial soil. Prior to this water holding capacity (WHC) of the artificial soil was determined. In order to provide the same percentage of the WHC in all the test concentrations, dilution of the irradiated solution was required before any bioassay. Each replicate consisted of a cylindrical plastic box (7 × 7 × 6 cm) divided in two halves by a transversally inserted card divider. Control soil was combined with all doses (2.27, 1.00, 0.74, 0.61 and 0.30 mg/kg). Therefore, each replicate included a control side and a half with contaminated soil. After soil addition, the divider was removed and 20 springtails were carefully placed on the midline of each test vessel. The tests ran under a photoperiod of 16 hr light:8 hr dark, at (20 ± 2)°C . During the test period (48 hr), every test chamber was covered by a transparent lid to prevent evaporation.

2 Results and discussion

2.1 Characterization of raw and P-modified TiO_2

2.1.1 Concentrations of P species distributed in TiO_2

Table 1 summarizes the P content of P-modified TiO_2 determined by ICP-AES analyses. As shown, the P/Ti ratios are a little higher than those adopted during preparation. This is due to the loss of water (dehydra-

Table 1 Chemical composition of P-modified TiO_2 samples

Sample	Atomic ratio (P/Ti)	
	Calculated	Measured
$TP8_{500}$	0.08	0.087
$TP5_{500}$	0.05	0.054
$TP2.5_{500}$	0.025	0.028

tion/dehydroxylation) and alcohol (adsorbed solvent in course of preparation of catalyst) during heat treatment. Similar types of observation are reported by Samantaray and Parida (2001).

2.1.2 Structural analysis

The changes of phase structure of the as-prepared catalysts after heat treatment at different temperatures are shown in Fig. 2. TP8, TP5, TP2.5 and TP0 calcined at various temperatures reveals anatase TiO_2 and were confirmed by comparing them with (JPCDS #84-1286) standard files. The peak intensity of anatase increases, and the width of the (101) plane diffraction peak of anatase at 25.4° becomes narrower with the increase of calcination temperature and the decrease of phosphate content. By contrast, the TP0 does not persist and the rutile becomes the only phase beyond 700°C (PCPDF #83-2242). This indicates a decrease in anatase content and a reduction in crystallite size. Based on the above results, we suggest that the thermal stability of anatase P-modified TiO_2 can be attributed to a main reason as the inhibition of crystalline grain growth of anatase TiO_2 by the dispersion of phosphate embedded with TiO_2 anatase phase. At high temperature calcination, $TP8_{900}$ and $TP5_{900}$ still show anatase phase and a new crystalline TiP_2O_7 (JCPDS #38-1468) with cubic lattice phase comes into being at the same time with anatase $TP8_{900}$ and $TP5_{900}$ (Yu, 2007; Lv et al., 2009). This new high temperature phase shows two main XRD at 2θ: 22.55 and 27.70° and is confirmed by comparing with PCPDF #38-1468.

Average crystalline sizes of all materials can be calculated from the broadening of (101) peak of anatase and (110) peak of rutile, as shown in Fig. 3 inset. For $TP0_{500}$, the average crystalline size of anatase (21 nm) quickly increases at temperatures above 500°C, indicating the sintering of TiO_2 particles at high temperature and the rutile phase becomes the only phase beyond 500°C. However, for $TP8_{500}$, the crystallite size of anatase is less than 10 nm. This is followed by limited change in particle growth till 700°C. At above this temperature, an increase in anatase particle size is observed, becoming significant

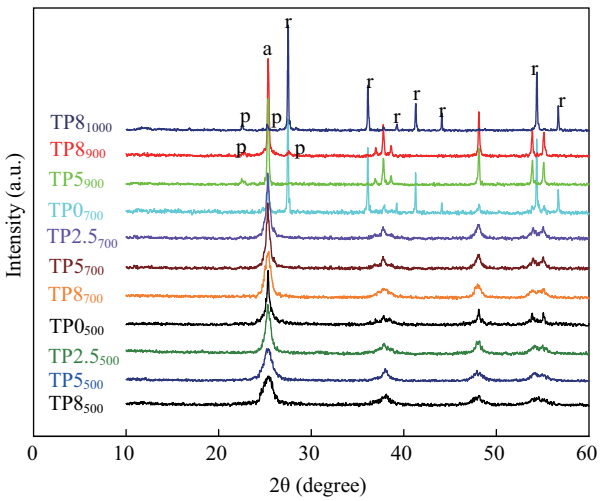

Fig. 2 XRD patterns of TP0, TP5, TP2.5 and TP8 calcined at various temperatures. a, r and p denote anatase, rutile and TiP_2O_7, respectively.

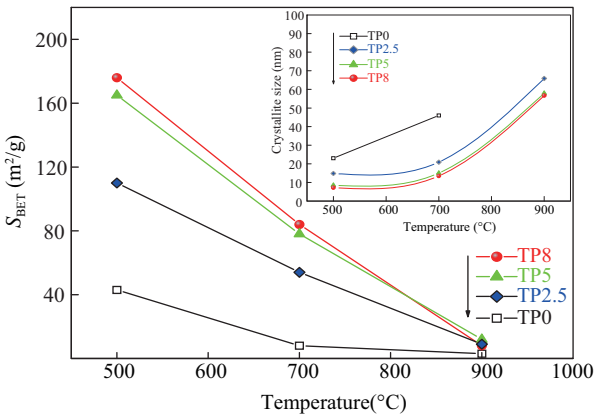

Fig. 3 Specific surface areas and average crystallite sizes (inset) of the samples calcined at various temperature. The average crystallite sizes are calculated from the broadening degree of (101) XRD peak of anatase phase.

at 900°C reflecting increased sintering. Therefore, it is creditable to attribute this behaviour of materials to the phosphate in the titania grain boundaries of TiO_2, avoiding direct contact and growth of the anatase particles and slows down the phase transition of anatase as reported by Zheng et al. (2008) and Li et al. (2009).

The BET surface areas of samples calcined at various temperatures are summarized in Fig. 3. As shown, with the increase of calcination temperature, the measured specific surface areas are opposed to the calculated crystallite size, indicating the crystallite growth of anatase during calcination. Upon calcination at 500–700°C, the surface area of $TP0_{500}$ is quickly decreased to 5 m^2/g, reflecting the loss of coordinated water and sintering of rutile $TP0_{700}$ particles (Ragai, 1985). This is corroborated by the thermal behaviour of the samples, as well as the infrared spectra. In contrast, anatase $TP8_{500}$, $TP5_{500}$ and $TP2.5_{500}$ are larger than that of the anatase $TP0_{500}$. This finding indicates that phosphorus-modified TiO_2 surface has more hydroxyl groups than raw TiO_2 which may be attributed to the less loss of water during calcination temperature on the one hand and the development of the bidentate state of phosphate groups on the surface of TiO_2, on the other (as revealed by FT-IR spectra). Above 700°C, a decrease in surface area is observed for doped TiO_2, becoming significant at 900°C. This is a reflection of loss of coordinated water, followed by sintering of anatase particles at higher temperatures.

The FT-IR spectra of raw and P-modified TiO_2 samples calcined at various temperatures are shown in Fig. 4. For all samples, the broad peak at 1630 and 3420 cm^{-1} corresponds to bending and asymmetric stretching modes of molecular water, respectively. These absorption bands assigned to strongly hydrogen bonded H–O–H is believed to be due to surface-adsorbed water and hydroxyl groups. Obviously, the P-modified samples have more surface-adsorbed water and hydroxyl groups than raw TiO_2 ($TP0_{500}$). The absorption bands increases as the P/Ti atomic ratio increases and decreases gradually with heating at a higher temperature. The bond at 1100 cm^{-1} is assigned to Ti–O–P vibrations that correspond to the phosphorus in the frame of TiO_2. The intensity of absorption peak (1100

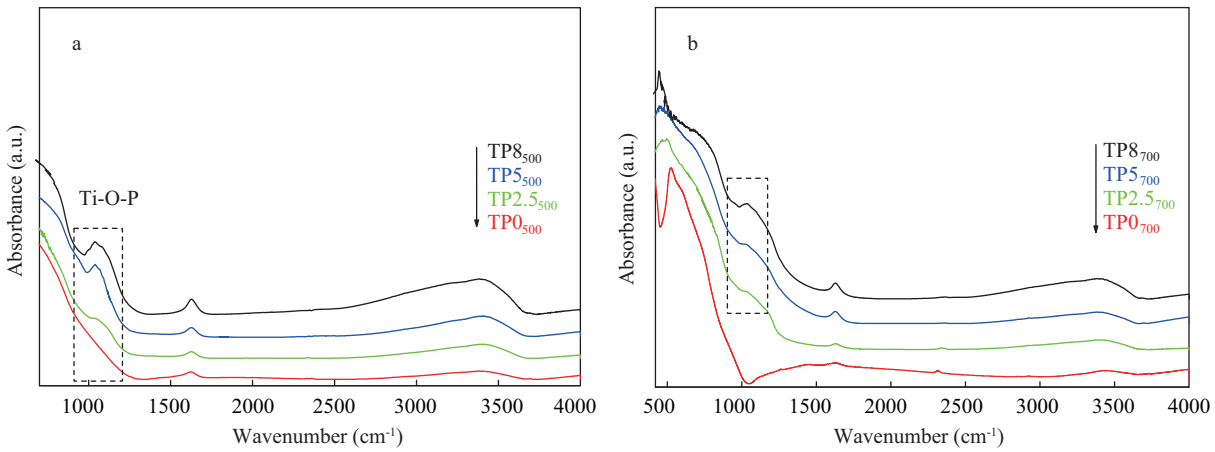

Fig. 4 FT-IR spectra of TP8, TP5, TP2.5 and TP0 calcined at 500°C (a) and 700°C (b).

cm^{-1}) turns stronger may be result form the increasing concentration of phosphorus content in TiO_2 structure (Fan et al., 2008; Ren et al., 2006; Connor and McQuillan,1999).

2.2 Photocatalytic degradation of 4-chlorophenol

2.2.1 Influence of P/Ti ratio on the photocatalytic properties P-modified TiO_2

Figure 5a shows the relative concentration of 4-chlorophenol and the release of chloride ions, after different UV-irradiation times. Nearly 88%, 84%, 78%, 47%, and 74% of 4-chlorophenol was degraded and about 74%, 68%, 60%, 38% and 55% of chlorine were removed by using respectively TP5, TP8, TP2.5, TP0 catalysts calcined at 500°C and Degussa P25 within the same irradiation time (270 min). The release of chloride ions is easily understood because the breaking of C–Cl bond is energetically more favourable than that of C–OH bond (the bond dissociated energy for C–Cl bond is approximately 10 kcal/mol less than that for C–OH bond (Boncz et al., 1997).

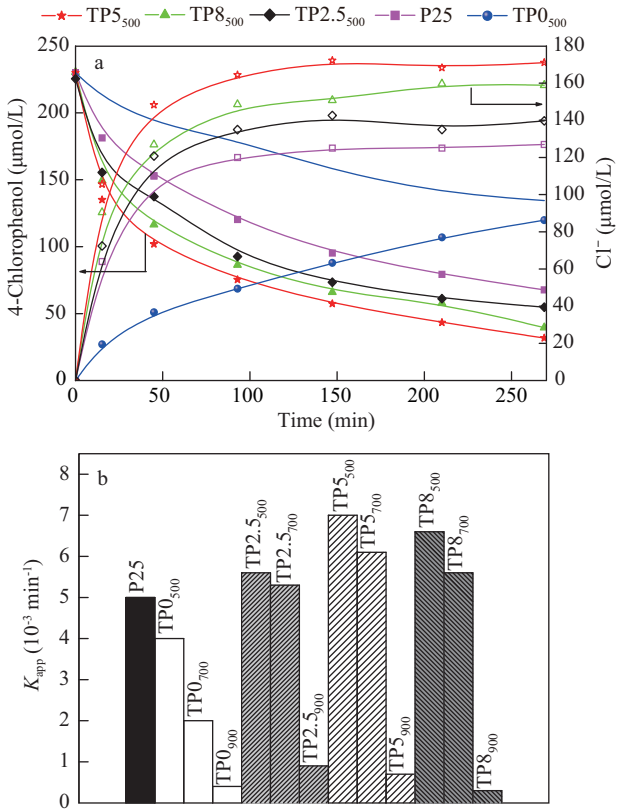

Fig. 5 (a) Typical curves of the degradation of 4-chlorophenol (solid symbols), release concentration of chloride ions (blank symbols) under UV irradiation, (b) the dependence of the apparent rate constants k_{app} at various temperatures under UV 0.23 mmol/L, TiO_2 1.5 g.

From these results it is clear that the P-modified TiO_2 calcined at 500°C shows the highest photocatalytic degradation activity than P25 and TP0 calcined at the same temperature. In addition, the catalyst with P/Ti ratio equal to 0.05 shows the highest photocatalysis activity, but increasing P/Ti ratio is not favourable to enhance the efficiency of degradation. Comparison of the structural parameters of samples TP5 and TP8 reveals that $TP8_{500}$ shows the highest surface area whereas its anatase content is lower than the corresponding value of $TP5_{500}$. Although higher phosphorus contents allow the synthesis of samples with larger surface areas, because of their decreased anatase contents, these may have lower photoactivities. It is therefore not expedient to increase the P/Ti atomic ratio to > 0.08. Similar observation are also reported earlier by Kõrösi et al. (2007). The high photocatalytic efficiency of the P-modified TiO_2 can be attributed to the reconstructed favorable structure with the incorporated P–O–Ti bonds and their new structure with quantum size (Hoffman et al., 1995) and high surface area, which is able to facilitate adsorption of water contaminants and effective utilization of UV light irradiation

2.2.2 Influence of calcination temperature on photocatalytic properties of P-modified TiO_2

As shown in Fig. 5b, the degradation of 4-chlorophenol decreases along with the increase of calcination temperature. Meanwhile, TP8, TP5 and TP2.5 still display a good photocatalytic activity at an elevated temperature up to about 700°C. When the calcination temperature increases to 900°C, the rate constant is significantly decreased for all catalysts. In contrast, the TP0 catalyst displays a poor photocatalytic activity at 700°C due to the smaller surface area, large crystalline size and anatase-rutile phase transformation.

2.2.3 UV–Vis spectrum of 4-chlorophenol during degradation

Figure 6a shows the absorbance changes at 225 and 280 nm of 4-chlorophenol on TP5 photocatalyst calcined at 500°C. These peaks gradually diminished with increasing irradiation time. The appeared broad absorption peak near 290 nm may possibly consist of the combination from 4-chlorophenol and some intermediates such as hydroquinone (221 and 290 nm) and benzoquinone (246 nm). These intermediates are then degraded by cleavage of their aromatic ring (Vinodgopal et al., 1993; Zang et al., 1995).

2.2.4 Intermediate pathways in the photocatalytic degradation of 4-chlorophenol

During the photocatalytic degradation with every catalyst, the aromatic intermediates were detected by HPLC. All the species in the solution were identified by the comparison of the retention times of the observed peaks with the retention times of standard HPLC peaks. For the studied catalyst, three intermediates were generated during the 4-chlorophenol degradation which are hydroquinone, benzoquinone and 4-chlorocatechol. It is well known that benzoquinone, hydroquinone and hydroxybenzoquinone are the major intermediates in the TiO_2 photocatalytic degradation of 4-chlorophenol (Moonsiri et al., 2004). The concentration of hydroquinone initially increased linearly with the degradation of 4-chlorophenol (Fig. 6b). After the disappearance of 74% of 4-chlorophenol, the concentration of hydroquinone reaches the maximum and the ratios of hydroquinone to the degraded 4-chlorophenol was kept about 14%, Thus, hydroquinone is a primary formed product from the degradation of seven 4-chlorophenol molecules. After 180 min of irradiation, the concentration of this major intermediate underwent a fast drop, indicating the mineralization of 4-chlorophenol. Our result is similar to that published for phosphated modified titania by Zhao et al. (2008). They compared the formation of hydroquinone in the photodegradation of 4-chlorophenol using phosphate-modified TiO_2 photocatalysts at UV-irradiated H_2O_2 system. The later system is known to form free hydroxyl radical OH through the photolysis of H_2O_2 by UV irradiation. They found that the hydroquinone is a primary formed product in the UV-H_2O_2 system. The similarity in the formation and disappearance tendency of hydroquinone between the P-modified TiO_2 and H_2O_2-UV systems implies that the degradation of 4-chlorophenol undergoes similar pathway in these two systems, and is initiated primarily from the free hydroxyl radical OH attack in the former system. Hence, we can suggest that the relatively high concentration of hydroquinone should be explained as originating from the free hydroxyl in the P-modified TiO_2 system

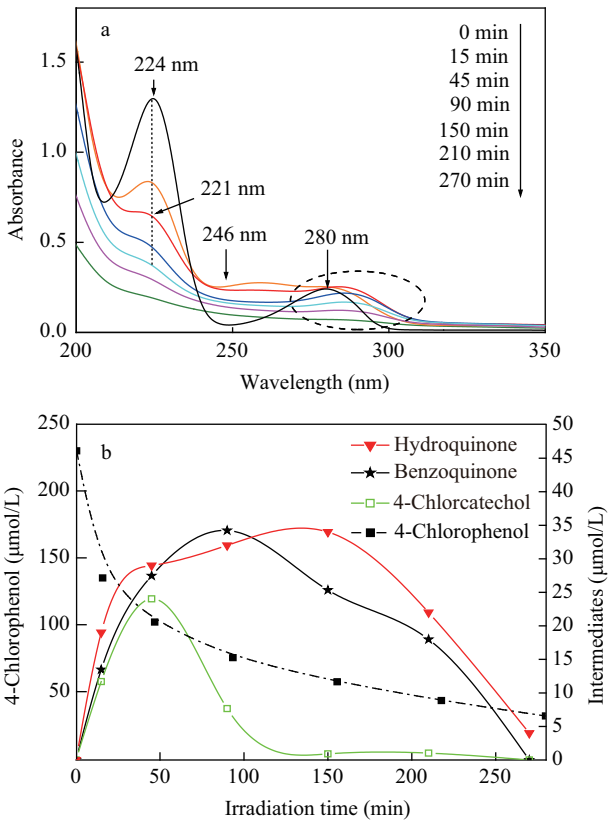

Fig. 6 (a) UV–Vis absorption spectra depicting the degradation profile of 4-chlorophenol using $TP5_{500}$; (b) variations in the concentration of 4-chlorophenol and the hydroxylated products from the photocatalytic degradation of 4-chlorophenol as a function of reaction time under UV illumination.

2.2.5 Mineralization of 4-chlorophenol

The extent of 4-chlorophenol mineralization on the TP5 photocatalyst calcined at 500°C is monitored by COD and TOC removal depicted in Fig.7a. The formation of organic intermediates by oxidation can decrease COD value in the irradiated solution, in the same time TOC values decrease slowly because organic intermediates are deeply oxidized to CO_2. It can be also observed that the COD reduction is slower up to about 87% and 13% COD remained in solution within 270 min. This may be because hydroquinone decomposition is related to a keto-enolic oxydo-reductive tautomeric effect as reported in previous work both from our laboratory and from other research group (Ksibi et al., 2003). Due to this effect, the oxidation of hydroquinone to benzoquinone by photo-generated holes (h^+) formed in the valence band of the TiO_2 semiconductor can be followed by the capture of an electron of the band of conduction by the benzoquinone, giving place to a reaction of recombination. Hence, the mineralization of hydroquinone by photocatalytic degradation is rather difficult (Chen et al., 2004; Venkatachalam et al., 2007).

2.2.6 Biodegradability enhancement of 4-chlorpheneol solution by photocatalysis

Figure 7b shows a significant decreases of COD of the treated solution, indicating that the intermediate products such as carboxyl acids are formed from parent compound and complete oxidation of 4-chlorophenol occurs. The COD value of initial solution is equal to 68 mg/L and the BOD_5 is close to zero which implies high toxicity to microorganisms in the environment. After treatment of the 4-chlorophenol solution for three hours, a fast increase of BOD_5 was observed. This finding is connected to the small quantity of hydroxylated intermediate (hydroguinone and

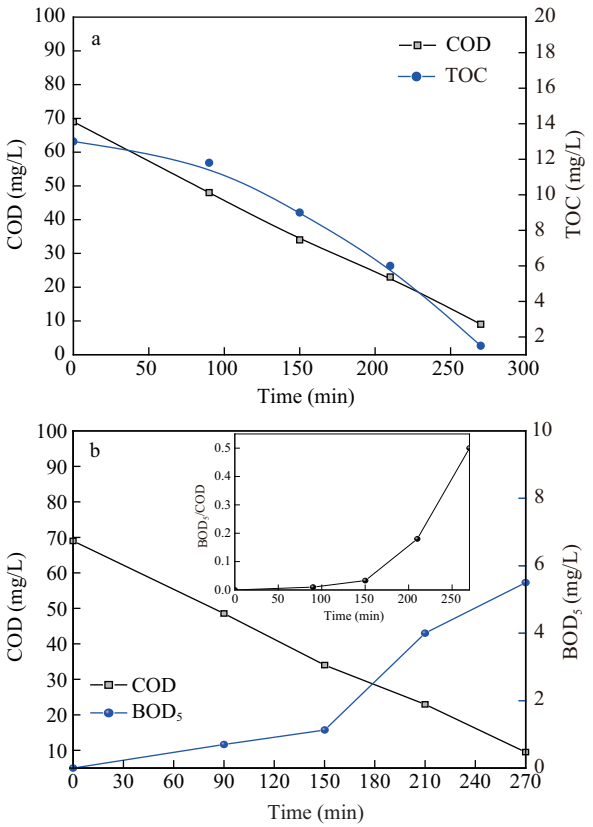

Fig. 7 (a) Changes in total organic carbon (TOC) and chemical oxygen demand (COD); (b) changes in BOD_5, COD, and biodegradability (as measured by BOD_5/COD ratios) of 4-chlorophenol concentration as a function of reaction time under UV illumination, using $TP5_{500}$ catalyst.

benzoquinone) that may be easily biodegraded as the reason for enhancement of biodegradability (Rao et al., 2003). The inset in Fig. 7b shows an increasing in ratio of BOD_5/COD versus irradiation time. All the photo-treated solutions which we evaluated the ratios BOD_5/COD show values higher than those recorded in initial solutions which is an indication of the positive effect of the applied photo-treatment. Thus, at 270 min of degradation time under UV light irradiation, the BOD_5/COD ratio of 0.5 suggested that adequately treated 4-chlorophenol solutions are biodegradable in contrast to untreated 4-chlorophenol solutions. Hence, our data indicated that the photocatalytic oxidation technique could be useful as a pre-treatment technique for reducing toxicity of toxic/hazardous wastewaters by improving the biodegradability (Hong and Zeng, 2002).

2.3 Phytotoxicity

Phytotoxicity tests were conducted to assess the impact of irradiated solution release to the environment as well as to evaluate the possible use of the pre-treated aqueous solution in the irrigation field. Indeed, this practice can alleviate the burden on underground water overexploitation and promote the practice of using treated water to irrigate golf courses, parks and gardens. Phytotoxicity of raw and treated 4-chlorophenol solution was tested using a seed germination assay and are depicted in Fig. 8. The seed germination in the tomato (*Lycopersicon esculentum*) was strongly inhibited by raw solution or with a photocatalysis duration (45 min) reflecting the recalcitrant nature of 4-chlorophenol. However, as photocatalysis progressed, a fast increase of germination index was observed. This fact is due to the small quantity of hydroxylated intermediate that may be easily biodegraded, is the reason for enhancement of biodegradability. At 270 min, the germination index reaches a maximum (75%). the toxicity of the treated solutions fell within the non-toxic range (Wang et al., 2001; Tamer et al., 2006). These results suggest that photocatalytic degradation is able to remove the phytotoxicity of 4-chlorophenol aqueous solution. Anyhow, the germination of seeds could help promoting the reuse of the treated water.

2.4 Acute toxicity

In the avoidance tests with the springtails no mortality was observed. Significant statistical differences were found between OECD soil and OECD modified soils by adding different samples of 4-chlorophenol phototreated solutions (Fig. 9).

A clear preference pattern for soil mixed with 4-chlorophenol solutions treated for long time by TiO_2-photocatalysis process in relation to OECD soil was observed, especially in the highest one (270 min). The *Folsomia candida* exhibited statistically significant ($p \leqslant 0.05$) avoidance of soils with higher 4-chlorophenol content when exposed in contaminated soils. In the "dual control test"; comparing OECD soil vs. OECD soil; no

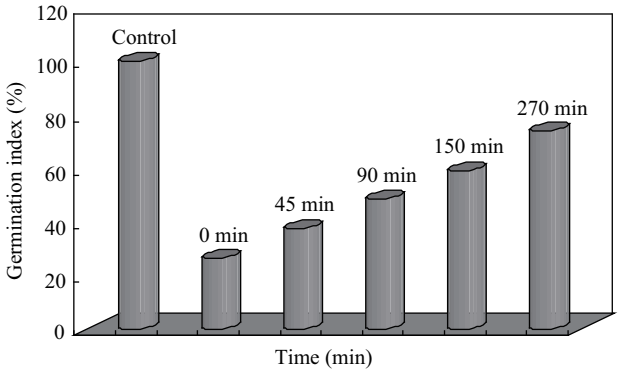

Fig. 8 Germination index as a function of reaction time under UV illumination, using $TP5_{500}$ catalyst.

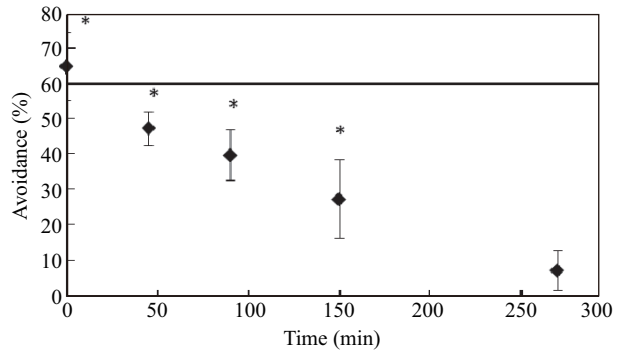

Fig. 9 Avoidance responses of *F. candida* to OECD artificial soil contaminated by residual 4-chlorophenol solutions irradiated during 45; 90; 150 and 270 min. * Indicates statistical differences ($p < 0.0001$) by the Fischer's Exact test, i.e., a significant avoidance response of the test soil. Data points above the dotted line indicate limited habitat function of the respective soil, according to the Hund-RInke criteria (Hund-Rinke et al., 2005). Data are expressed as average ±SD.

statistical difference was found. This indicates the homogeneous distribution of the springtails between the two sides of the test chamber. It can be noted that in the first 60 min of irradiation, there was a significant fluctuation of the avoidance of springtails. This behavior could be correlated to intermediates formed during the degradation. It is believed that this phenomenon can be attributed to substances, generated in very low concentrations, and presenting a high level of toxicity. No intermediates, in the concentrations in which they were generated in the reaction mixture, presented a higher toxicity than the parent compound (4-chlorophenol). Photocatalysis was quite efficient in removing toxicity. The 48 hr EC_{50} value determined statistically for 4-chlorophenol was 1.21 mg/kg in the present study. EC_{50} values are useful as a relative toxicity screening evaluation to estimate which chemicals or liquids have a greater toxicity potential. Low EC_{50} values indicate a higher toxicity potential and high EC_{50} values indicate a lower toxicity. Thus, as toxicity is reduced, EC_{50} values increase. As a point of reference, EC_{50} values published by Dassapa and Loehr (1991), indicate that phenol (EC_{50} = 26.7) had a lower toxicity potential than p-cresol (EC_{50} = 1.1) (Glaze, 1994). The original 4-chlorophenol solution is highly toxic to *Folsomia candida* since the EC_{50} value is very low. Indeed, it is necessary to eliminate it from industrial wastewater before discharge.

3 Conclusions

The photocatalytic degradation of 4-chlorophenol using different catalysts, TiO_2 (Degussa P25), TiO_2 (sol-gel), P-modified TiO_2 (sol-gel), was investigated. On the basis of the described results we can conclude that the photocatalytic activity under UV irradiation of P-modified TiO_2 (TP5) was 4.5 folds higher than that of raw TiO_2 and was 23% higher than that of commercial Degussa P-25. The main intermediate products generated during the photocatalytic reaction were found to be hydroquinone, benzoquinone and 4-chlorocatechol. Considering the potential effect of some of these compounds on the ecosystem, phytotoxicity to tomato (*Lycopersicon esculentum*) seeds and acute toxicity by using *Folsomia candida* as the test organism were successfully applied in ecological risk assessment of 4-chlorophenol phototreated solutions. The toxicological assays showed a significant reduction of toxicity after 4-chlorophenol photocatalytic degradation, indicating that this process corresponds to an actual detoxification of 4-chlorophenol.

Acknowledgments

We are grateful to the Ministry of Higher Education, Scientific Research and Technology the financial support to the current work.

References

Bickley R I, Gonzalez-Carreno T, Lees J S, Palmisano L, Tilley R J D, 1991. A structural investigation of titanium dioxide photocatalysts. *Journal of Solid State Chemistry* 92(1): 178–190.

Boncz M A, Bruning H, Rulkens W H, Sudholter E J R, Harmsen G H, Bijsterbosch J W, 1997. Kinetic and mechanistic aspects of the oxidation of chlorophenols by ozone. *Water Science and Technology*, 35(4): 65–72.

Chang S M, Hou C Y, Lo P H, Chang C T, 2009. Preparation of phosphated Zr-doped TiO_2 exhibiting high photocatalytic activity through calcination of ligand-capped nanocrystals. *Applied Catalysis B: Environmental*, 90(1-2): 233–241

Chen C C, Lei P X, Ji H W, Ma W H, Zhao J C, Hidaka H et al., 2004. Photocatalysis by Titanium dioxide and polyoxometalate/TiO_2 cocatalysts. Intermediates and mechanistic study. *Environmental Science and Technology*, 38(1): 329–337.

Chen D W, Ray A K, 1999. Photocatalytic kinetics of phenol and its derivatives over UV irradiated TiO_2. *Applied Catalysis B: Environmental*, 23(2-3): 143–157.

Chen H R, Shi J L, Hua Z L, Ruan M L, Yan D S, 2001. Parameter control in the synthesis of ordered porous zirconium oxide. *Materials Letters*, 51(3): 187–193.

Cheng Y P, Sun H Q, Jin W Q, Xu N P, 2007. Photocatalytic degradation of 4-chlorophenol with combustion synthesized TiO_2 under visible light irradiation. *Chemical Engineering Journal*, 128(2-3): 127–133.

Connor P A, McQuillan A J, 1999. Phosphate adsorption onto TiO_2 from aqueous solutions: an *in situ* internal reflection infrared spectroscopic study. *Langmuir*, 15(8): 2916–2921.

Dassapa S M, Loehr R C, 1991. Toxicity reduction in contaminated soil bioremediation processes. *Water Research*, 25(9): 1121–1130.

Ding Z, Lu G Q, Greenfield P F, 2000. Role of the crystallite phase of TiO_2 in heterogeneous photocatalysis for phenol oxidation in water. *The Journal of Physical Chemistry B*, 104(19): 4815–4820.

EEC Directive, 1990. European Community. *Brussels* 80/778/EEC 15-7-1990.

Fan X X, Yu T, Wang Y, Zheng J, Gao L, Li Z S et al., 2008. Role of phosphorus in synthesis of phosphated mesoporous TiO_2 photocatalytic materials by EISA method. *Applied Surface Science*, 254(16): 5191–5198.

Fujishima A, Rao T N, Tryk D A, 2000. Titanium dioxide photocatalysis. *Journal of Photochemistry and Photobiology C: Photochemistry Reviews*, 1(1): 1–21.

Gerischer H, Heller A, 1992. Photocatalytic oxidation of organic molecules at TiO_2 particles by sunlight in aerated water. *Journal of the Electrochemical Society*, 139(1): 113–118.

Glaze W H, 1994. An overview of advanced oxidation processes: Current status and kinetic models. In: Chemical Oxidation: Technologies for the Nineties Proceedings of the third International Symposium: Chemical Oxidation: Technology for the Nineties (Eckenfelder W W, Bowers A R, Roth J A, eds.). Technomic Publishing Company. Tennessee, NV, Lancaster. 17–19 February. Vol: 3.

Herrmann J M, Matos J, Disdier J, Guillard C, Laine J, Malato S et al., 1999. Solar photocatalytic degradation of 4-chlorophenol using the synergistic effect between titania and activated carbon in aqueous suspension. *Catalysis Today*, 54(2): 255–265.

Hoffmann M R, Martin S T, Choi W, Bahnemann D W, 1995. Environmental applications of semiconductor photocatalysis. *Chemical Reviews*, 95(1): 69–96.

Hong P K A, Zeng Y, 2002. Degradation of pentachlorophenol by ozonation and biodegradability of intermediates. *Water Research*, 36(17): 4243–4254.

JIS (Japanese Industrial Standard Handbook), 1998. Environmental technology testing method for industrial wastewater, Japanese Standard Association.

Komilis D P, Karatzas E, Halvadakis C P, 2005. The effect of olive mill wastewater on seed germination after various pretreatment techniques. *Journal of Environmental Management*, 74(4): 339–348.

Kõrösi L, Papp S, Bertóti I, Dékány I, 2007. Surface and bulk composition, structure, and photocatalytic activity of phosphate-modified TiO_2. *Chemistry of Material*, 19(19): 4811–4819.

Ksibi M, Zemzemi A, Boukchina R, 2003. Photocatalytic degradability of substituted phenols over UV irradiated TiO_2. *Journal of Photochemistry and Photobiology A: Chemistry*, 159(1): 61–70.

Li F F, Jiang Y S, Xia M S, Sun M M, Xue B, Liu D R et al., 2009. Effect of the P/Ti ratio on the visible-light photocatalytic activity of P-doped TiO_2 *Journal of Physical Chemistry C*, 113(42): 18134–18141.

Lv Y Y, Yu L S, Huang H Y, Liu H L, Feng Y Y, 2009. Preparation, characterization of P-doped TiO_2 nanoparticles and their excellent photocatalytic properties under the solar light irradiation. *Journal of Alloys and Compounds*, 488(1): 314–319.

Moonsiri M, Rangsunvigit P, Chavadej S, Gulari E, 2004. Effects of Pt and Ag on the photocatalytic degradation of 4-chlorophenol and its by-products. *Chemical Engineering Journal*, 97(2-3): 241–248.

Peng P, Wang H J, Yu H, Chen S H, 2006. Preparation of aluminum foil-supported nano-sized ZnO thin films and its photocatalytic degradation to phenol under visible light irradiation. *Materials Research Bulletin*, 41(11): 2123–2129.

Pera-Titius M, García-Molina V, Baños M A, Giménez J, Esplugas S, 2004. Degradation of chlorophenols by means of advanced oxidation processes: a general review. *Applied Catalysis B: Environmental* 47(4): 219–256

Poulios I, Makri D, Prohaska X, 1999. Photocatalytic treatment of olive milling waste water: oxidation of protocatechuic acid global. *GLOBAL NEST: the International Journal*, 1(1): 55–62.

Ragai J, 1985. Ageing studies on some titania gels. *Journal of Chemical Technology and Biotechnology*, 35(5): 263–269.

Rao N N, Dubey A K, Mohanty S, Khare P, Jain R, Kaul S N, 2003. Photocatalytic degradation of 2-chlorophenol: a study of kinetics, intermediates and biodegradability. *Journal of Hazardous Materials*, 101(3): 301–314.

Ren T Z, Yuan Z Y, Azioune A, Pireaux J J, Su B L, 2006. Tailoring the porous hierarchy of titanium phosphates. *Langmuir*, 22(8): 3886–3894.

Samantaray S K, Parida K, 2001. Effect of phosphate ion on the textural and catalytic activity of titania-silica mixed oxide. *Applied Catalysis A: General*, 220(1-2): 9–20.

Scott J P, Ollis D F, 1995. Integration of chemical and biological oxidation processes for water treatment. *Environment Program*, 14(2): 88–103.

Tamer E, Hamid Z, Aly A M, Ossama E T, Bo M, Benoit G, 2006. Sequential UVbiological degradation of chlorophenols. *Chemosphere*, 63(2): 277–284.

Tanaka K, Capule M F V, Hisanga T, 1991. Effect of crystallinity of TiO_2 on its photocatalytic action. *Chemical Physics Letters*, 187(1-2): 73–76.

US EPA, 1987. Federal Register. Washington DC, 52, 131, 25861–25962.

Venkatachalam N, Palanichamy M, Arabindoo B, Murugesan V, 2007. Enhanced photocatalytic degradation of 4-chlorophenol by Zr^{4+} doped nano TiO_2. *Journal of Molecular Catalysis A: Chemical*, 226(1-2): 158–165.

Vinodgopal K, Hotchandani S, Kamat P V, 1993. Electrochemically assisted photocatalysis: titania particulate film electrodes for photocatalytic degradation of 4-chlorophenol. *The Journal of Physical Chemistry*, 97(35): 9040–9044

Wang X D, Sun C, Gao S X, Wang L S, Han S K, 2001. Validation of germination rate and root elongation as indicator to assess phytotoxicity with *Cucumis sativus. Chemosphere*, 44(8): 1711–1721.

Yu H F, 2007. Photocatalytic abilities of gel-derived P-doped TiO_2. *Journal of Physics and Chemistry of Solids*, 68(4): 600–607.

Yu J C, Zhang L Z, Zheng Z, Zhao J C, 2003. Synthesis and characterization of phosphated mesoporous titanium dioxide with high photocatalytic activity. *Chemistry of Material*, 15(11): 2280–2286.

Zang L, Liu C Y, Ren X M, 1995. Photochemistry of semiconductor particles. Part 4. Effects of surface condition on the photodegradation of 2, 4-dichlorophenol catalysed by TiO_2 suspensions. *Journal of the Chemical Society Faraday Transactions*, 91(5): 917–923.

Zhao D, Chen C C, Wang Y F, Ji H W, Ma W H, Zang L et al., 2008. Surface modification of TiO_2 by phosphate: Effect on photocatalytic activity and mechanism implication. *Journal of Physical Chemistry C*, 112(15): 5993–6001.

Zheng R Y, Lin L, Xie J L, Zhu Y X, Xie Y C, 2008. State of doped phosphorus and its influence on the physicochemical and photocatalytic properties of p-doped Titania. *Journal of Physical Chemistry*, 112(39): 15502–15509.

Zucconi F, Pera A, Forte M, De Bertoldi M, 1981. Evaluating toxicity of immature compost. *Biocycle*, 22(2): 54–57.